Advances in Materials Research, *Vol. 8, No. 4 (2019) 337-359*
DOI: https://doi.org/10.12989/amr.2019.8.4.337

Flexural analysis of thermally actuated fiber reinforced shape memory polymer composite

Nilesh Tiwari * and A.A. Shaikh [a]

Mechanical Engineering Department, S.V. National Institute of Technology, Surat-395007, India

(*Received September 18, 2019, Revised January 5, 2020, Accepted February 12, 2020*)

Abstract. Shape Memory Polymer Composites (SMPC) have gained popularity over the last few decades due to its flexible shape memory behaviour over wide range of strains and temperatures. In this paper, non-linear bending analysis has been carried out for SMPC beam under the application of uniformly distributed transverse load (UDL). Simplified C^0 continuity Finite Element Method (FEM) based on Higher Order Shear Deformation Theory (HSDT) has been adopted for flexural analysis of SMPC. The numerical solutions are obtained by iterative Newton Raphson method. Material properties of SMPC with Shape Memory Polymer (SMP) as matrix and carbon fibre as reinforcements, have been calculated by theory of volume averaging. Effect of temperature on SMPC has been evaluated for numerous parameters for instance number of layers, aspect ratio, boundary conditions, volume fraction of carbon fiber and laminate stacking orientation. Moreover, deflection profile over unit length and behavior of stresses across thickness are also presented to elaborate the effect of glass transition temperature (T_g). Present study provides detailed explanation on effect of different parameters on the bending of SMPC beam for large strain over a broad span of temperature from 273-373K, which encompasses glass transition region of SMPC.

Keywords: SMP; SMPC; HSDT; FEM; glass transition region

1. Introduction

Smart materials have fascinated the researchers since the discovery of shape memory phenomenon in 1931 due to its unique and dynamic functional properties (Vernon and Vernon 1941). Even though these materials have been in use over last eight decades, noticeable applications spiked with the discovery of efficient NiTi Shape Memory Alloy (SMA) (Buehler *et al*. 1963). It can be programmed as per the application to regain its primary shape due to the transition of temperature between martensite and austenite phase (Yang 2000). In the past few decades, some alternatives are being explored to overcome limitations of SMA such as expense and poor fatigue. Among the various possible solutions Shape Memory Polymer (SMP) is a viable option and the further work is concentrated on it (Jani *et al*. 2014). SMPs are those material which can be temporarily deformed and recovered into original shape in the presence of external stimuli such as temperature (Koerner *et al*. 2013), mechanical stress (Heuwers *et al*. 2013), pH and moisture (Han *et al*. 2012), light (Lendlein *et al*. 2005), electricity (Cho *et al*. 2005) magnetism

*Corresponding author, Research Scholar, E-mail: nileshbwtiwari@gmail.com
[a] Professor, E-mail: aas.svr1@gmail.com

http://www.techno-press.org/?journal=amr&subpage=5 ISSN: 2234-0912 (Print), 2234-179X (Online)

(Mohr *et al*. 2006) or solvents (Quitmann *et al*. 2014). Among these stimuli, the present work has been confined to temperature.

Temperature activated SMPs have excellent shape memory property with appreciable shape recovery and shape fixity. However, variation of thermal conditions results in inferior mechanical properties of polymer due to its thermal degradation (Feldkamp and Rousseau 2010). Thus, to overcome the obstacle, composites have been developed with reinforcements of numerous nanoparticles and fibres (Leng *et al*. 2011). Shape memory property of polymers is slightly compromised with insertion of reinforcements but it can be negotiated with the considerable enhancement of the mechanical properties (Mu *et al*. 2018). SMPs are subjected with a wide range of strains as per application of material such as smart clothes (Oh *et al*. 2006), deployable space antennas and structures (Liu *et al*. 2014), artificial bones and cartilage in biomedical engineering (Rodriguez *et al*. 2012), electronic sensors (Ware *et al*. 2012) and various other applications.

The property of high recoverable strain of SMPs have allowed its application in the structures subjected to large stains such as deployable antennas (Xie and Rousseau 2009). Thus understanding of the material properties becomes critical for such applications. The behaviour of these materials can be understood with respect to static and dynamic properties of SMPs. Static properties mainly include ultimate tensile strength, yield stress, Young's modulus, Poisson's ratio and shear modulus (Li *et al*. 2016). Eminent dynamic property of SMPs consists of glass transition temperature (T_g) across which shape recovery and deformation of structure occurs. T_g can be estimated through dynamic mechanical analysis by Dynamic Mechanical Analyser (DMA) or Differential Scanning Calorimeter (DSC) (Mu *et al*. 2018, Li *et al*. 2016).

Currently, available literature demonstrates numerous examples of design and experiments of various SMP and shape memory polymer composites (SMPC) (Gu *et al*. 2018, 2019, Lu *et al*. 2017, Zhou *et al*. 2016, Kausar 2016, Guo *et al*. 2016, Wang *et al*. 2019a, b, Nurly *et al*. 2019, Li *et al*. 2019, Patel and Purohit 2019, Hassanzadeh-Aghdam *et al*. 2019, Gao *et al*. 2019, Quade *et al*. 2018). Existing literature based on experimental investigation, elaborates various mechanical tests performed on SMP structure with and without reinforcements (Kausar 2016, Guo *et al*. 2016). Tensile and compressive properties are sufficient for materials subjected to small strain (Quade *et al*. 2018). If the material is required to undergo large strain, as in the case of a deployable space antenna, then the bending test becomes a significant test (Li *et al*. 2019). Bending analysis explains the phenomena of deformation on the different locations of structure subjected to stress. Extreme loading conditions during the bending tests would also reveal the process of probable possibility of deflection, buckling or eventual failure of material (Li *et al*. 2019, Zhang and Ni 2007, Lan *et al*. 2014, Poilane *et al*. 2000).

Bending analysis of composite structures has been a point of extensive research subjected to different types of loading, but scarce work has been discovered for shape memory materials (Baghani *et al*. 2014, Li *et al*. 2019). Moreover, limited literatures focuse on the frontiers of analytical and numerical estimation of bending displacement with shape memory behaviour of SMP or SMPC (Zeng *et al*. 2018, Pearce *et al*. 2019, Su and Peng 2018). This is due to the fact that SMP has a broad range of mechanical characteristics in the vicinity for its discrete T_g. Thus it becomes difficult to analyse its behaviour in the glass transition zone. There are two widely accepted approaches to predict the shape memory behaviour of SMP and SMPC namely, the phase transition model and the thermo-viscoelastic model. Based on these models, the bending analysis of SMP structure has been rarely attempted (Lan *et al*. 2014, Baghani *et al*. 2014, Su and Peng 2018, Ghosh *et al*. 2013).

Li *et al*. (2019) determined the bending shape recovery properties of epoxy matrix SMP with

the variation of 16-37% carbon fiber reinforcement for the design and development of deployable space antennas. Relations of flexural stress, storage modulus, flexural strain and flexural modulus calculated with respect to temperature to gauge the effect on SMPC in the glass transition zone of material to evaluate the effect on mechanical behavior. Lan *et al*. (2009) carried out experimental and analytical study of micro-buckling phenomenon for carbon fibre reinforced epoxy shape polymer composites during bending tests. The model was derived with the assumption of material to be linearly elastic to calculate total energy, position and curvature of critical buckling, and wavelength and amplitude of buckled fibre. The experimental and corresponding theoretical work were found to be in reasonable agreement which paved the way for future analytical work with further sophistication. Zhang *et al*. (2018) also analytically derived the simplified expression to predict micro-buckling wavelength of Elastomeric Memory Composites (EMC) for the structure subject to large bending strains. Derived results were verified with previous analytical and experimental work by Lan *et al*. (2009) that estimated buckling behavior of composite with the consideration of 3D linear elastic solid through the finite strain of a plate with the energy method. Wang *et al*. (2010) developed a simplified analytical model to calculate micro-buckling of reinforcement in epoxy SMPC subjected to bending based on the minimum potential energy theory. The estimated buckling parameters were compared with analytical and experimental work by previous researchers (Campbell *et al*. 2004) which were found to be in reasonable convergence with corresponding reference data.

Baghani *et al*. (2014) presented the analytical solution of the SMP subjected to bending derived from Euler–Bernoulli beam theory and validated it with a prior work. (Liu *et al*. 2003). The model derived by Baghani *et al*. (2012) for SMP was employed to derive the analytical model to predict deflections during bending through FEM. Ghosh *et al*. (2013) produced a beam theory model to estimate the deflection of thermo-viscoelastic SMP based on continuum mechanics theory previously given by Ghosh and Srinivasa (2011). Three-point bending experiment was performed to verify FEM calculations for the application of theory in elastic, plastic and thermoplastic materials. Zhang and Ni (2007) estimated the influence of fiber orientation on bending recovery for polyurethane SMP and carbon fiber reinforced polyurethane SMPC along T_g to characterize shape memory property through DMA. SMPC with 0° fiber orientation had minimum recovery whereas SMPC with 90° fiber orientation had maximum recovery, which were also analytically verified with a simplified model.

He *et al*. (2017) studied the phenomenon of buckling in a silicon layered thin film on viscoelastic SMP substrate under the influence of bending and presented a FEM based simplified model. It was observed that the modulus of SMP drastically transformed in the ambience of T_g, as a result, it deformed under bending and compression without buckling. Wang and Li (2011) analyzed the bending behavior of SMP beam sandwiched between metallic films. SMP buckled due to the application of load above its critical value, which was even analytically reproduced through principle of total strain energy. Post buckling response in the form of failure had also been evaluated through different modes of failure. Poilane *et al*. (2000) employed non-conventional methods of characterizations such as nano-indentation; bulging and membrane point deflection tests to estimate mechanical properties of SMP thin film. Investigations performed at a normal temperature provided excellent results for bulging and nano-indentation, which might be insufficient to analyze shape memory behavior.

Finite element analysis of SMPC has been attempted mostly on commercial software which generally considers Classical Laminate Plate Theory or Euler-Bernoulli Beam Theory. In this paper, bending analysis is based on C° continuity Finite Element Method (FEM) and Higher Order

Shear Deformation Theory (HSDT) for modelling of the displacement field. Lal *et al*. (2007) applied C° continuity and HSDT to predict the behaviour of laminated composites under vibration. Material properties were estimated by Halpin-Tsai Method, which gave improved analysis as compared to previous work. Shi *et al*. (1998) applied third order shear deformation theory to study the behavior of laminated composites subjected to bending. Lal and Markad (2018) applied HSDT and C° continuity FEM to estimate bending displacement of particulate and fibre reinforced hybrid composites placed on elastic foundation.

Deformation analysis of 1-D SMPC beam subjected to transverse load with the consideration of glass transition region, especially analytical study based on Finite Element Method, has scarcely been stated in the literature. The present work offers a simplified C^0 continuity FEM based on HSDT through the principle of minimum potential energy approach to find deflections of carbon fiber reinforced SMPC with the first time implementation on shape memory phenomenon over the prescribed temperature region. The results have been obtained below as well as above glass transition region to evaluate the effect of temperature variation on SMPC beam. The effect of T_g has been studied with respect to different parameters such as number of layers, aspect ratio, boundary conditions, volume fraction of carbon fiber, sequence of laminate stacking with orientation of carbon fiber. Moreover, unit length deflection profile and layer-wise effect of stresses due to bending of the beam in the glass transition region are also demonstrated.

The paper is organized in the following sequence to calculate the non-linear bending deflection of SMPC. Section 1 discusses the brief significance of bending analysis of shape memory structures for large strain applications. Section 2 describes the material parameters of SMP matrix and carbon fiber, which combines to form SMPC. This is followed by the micromechanical modelling to evaluate properties of SMPC and a brief description of FEM formulation in this section. Section 3 analyses the results of transverse central deflection under uniformly distributed transverse loading for the parameters included in this work. Section 4 presents a summarized review of the results with its probable future application.

2. Calculation of model parameters

In this section, material properties of matrix, carbon fiber and SMPC are evaluated, which can be utilized to estimate the deflection of a beam subjected to transverse load (q_m). Model parameters are derived based on the characteristics of polymer matrix and carbon fiber reinforcements. The matrix selected in the current work is SMP with consideration of temperature's effect on its mechanical properties which are regulated by the glass transition temperature.

2.1 Modulus of SMP matrix

The material properties of SMP has been determined by researchers in the previous works. Extensive investigation of the SMP selected for the analysis has been done by Westbrook et al. (2011). Therefore, parameters required for the model can be experimentally investigated or obtained analytically by curve-fitting to experimental data (Gu *et al*. 2017).

A mathematical model is shown in Eq. (1) had been proposed to calculate values of storage modulus $E(T)$ of the polymers at a wide span of temperatures across T_g with a constant frequency (Mahieux and Reifsnider 2001).

$$E(T) = (E_1 - E_2).exp\left(-\left(\frac{T}{T_\beta}\right)^{m_1}\right) + (E_2 - E_3).exp\left(-\left(\frac{T}{T_g}\right)^{m_2}\right) + E_3.exp\left(-\left(\frac{T}{T_f}\right)^{m_3}\right) \quad (1)$$

where T is a wide range of temperature before and after T_g. E_1, E_2 and E_3 are material's moduli at the initiation of β-transition, glass transition and flow region respectively and T_β, T_g and T_f are the corresponding temperatures. m_1, m_2 and m_3 are Weibull exponents. The parameters to be substituted in Eq. (1) has been obtained from the work by Gu *et al*. (2017) summarized in Table 1. The values of the various parameters were experimentally obtained through Dynamic Mechanical Analysis. Fig. 1 has been plotted from Eq. (1) and its result is compared with the corresponding experimental data, which shows appreciable convergence. Storage modulus has been considered as Young's modulus in the subsequent analysis, as loss modulus is negligible as compared to storage modulus (Gu *et al*. 2019).

Table 1 Values of parameters in model for Epoxy SMP (Gu *et al.* 2017)

Notation	Description	Value
T_g	Glass transition temperature	305 K
T_m	Reference Temperature	300.5 K
T_β	β-transition temperature	295.2 K
T_f	Flow region temperature	415.5 K
E_1	Modulus at initiation of β-transition	2.552 GPa
E_2	Modulus at initiation of glass transition	1.876 GPa
E_3	Modulus at initiation of flow region	5 MPa
m_1, m_2, m_3	Weibull exponents	19.3, 58.4, 177.6
μ_g	Poisson's ratio of the frozen phase	0.35
μ_r	Poisson's ratio of the active phase	0.499
Z	Parameter characterizing the width of the phase transition zone	7

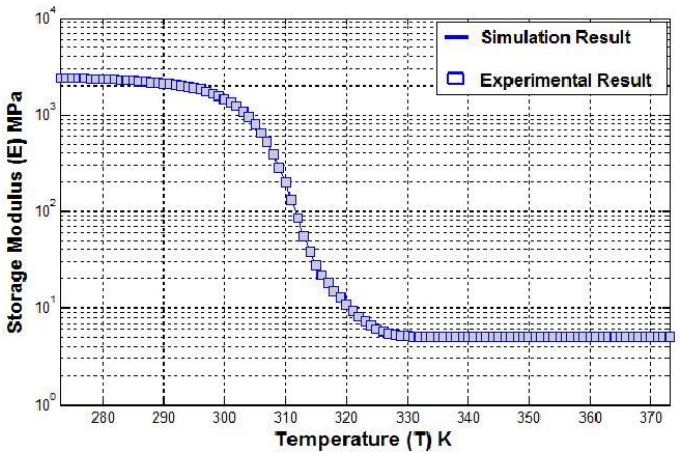

Fig. 1 Variation of Storage modulus with respect to temperature

Temperature dependent Poisson's ratio (μ) can be calculated through phase transition model for SMP material (Qi *et al*. 2008).

$$\mu = \mu_g v_g + \mu_r(1 - v_g) \tag{2}$$

$$v_g = 1 - \frac{1}{1 + exp\,[-(T - T_m)/Z]} \tag{3}$$

where $\mu_g\ and\ \mu_r$ are Poisson's ratio of the frozen and active phase respectively. v_g is the volume fraction of the frozen phase. T_m is reference temperature. *Z* is parameter characterizing the width of the phase transition zone. These mechanical parameters are utilized in the subsequent section to estimate the modulus of the SMPC beam subjected to variable temperature in the vicinity of T_g.

2.2 Material properties of fiber reinforced SMPC

The properties of composite material are estimated through the theory of volume averaging, as per the assumption that matrix and fiber have similar deformations (Shen *et al*. 2006). Following equations are utilized as per the theory to calculate numerous material properties.

$$E_{c1} = E_{f1} v_f + E_m v_m \tag{4}$$

$$E_{c2} = (1 - C)E_{c2}^1 + CE_{c2}^2 \tag{5}$$

$$\mu_{c21} = (1 - C)\mu_{c21}^1 + C\mu_{c21}^2 \tag{6}$$

$$\mu_{c12} = \mu_{c21}\frac{E_{c2}}{E_{c1}} \tag{7}$$

$$G_{c12} = (1 - C)G_{c12}^1 + CG_{c12}^2 \tag{8}$$

where E_{c1} and E_{c2} are modulus of composites along longitudinal and transverse directions respectively. E_{f1} and E_{f2} are Young's modulus of fiber along longitudinal and transverse directions respectively. G_{f12} is shear modulus along plane 1-2. G_{c12} is shear modulus of composite in 1-2 plane. C is transverse contact coefficient between fibers. μ_f is Poisson's ratio of carbon fiber. μ_{c12} and μ_{c21} indicate Poisson's ratio of composites along 1-2 and 2-1 plane respectively. The superscript 1 and 2 indicate values of constants in series and parallel respectively.

The material parameters of the composites are calculated with the values provided by analysis to estimate the properties of a matrix calculated from Eqs. (1), (2) and (3) for different temperatures. Data of material properties of carbon fiber has been referred from data provided by Shen *et al*. (2006), indicated in Table 2. The values of properties in series and parallel are estimated from the following equations, which will be substituted in Eqs. (4) to (8).

$$E_{c2}^1 = \frac{E_{f2}E_m}{E_{f2}v_m + E_m v_f} \tag{9}$$

$$E_{c2}^2 = E_{f2}v_f + E_m v_m \tag{10}$$

$$\mu_{c21}^{1} = \mu_f v_f + \mu_m v_m \tag{11}$$

$$\mu_{c21}^{2} = \frac{\mu_f E_{f2} v_f + \mu_m E_m v_m}{E_{f2} v_f + E_m v_m} \tag{12}$$

$$G_{c12}^{1} = \frac{G_{f12} G_m}{G_{f12} v_m + G_m v_f} \tag{13}$$

$$G_{c12}^{2} = G_{f12} v_f + G_m v_m \tag{14}$$

The results of longitudinal, transverse and shear modulus of SMPC are indicated in Figs. 2(a), (b) and (c) respectively. It can be noticed that as in the case of SMP, the material parameters of the SMPC drastically decline in the temperature range of glass transition region, indicating a sudden variation of properties of composites in the ambiance of T_g. The properties of SMPC are substituted in the following stages of FEM to determine deformation behavior under uniformly distributed transverse loading.

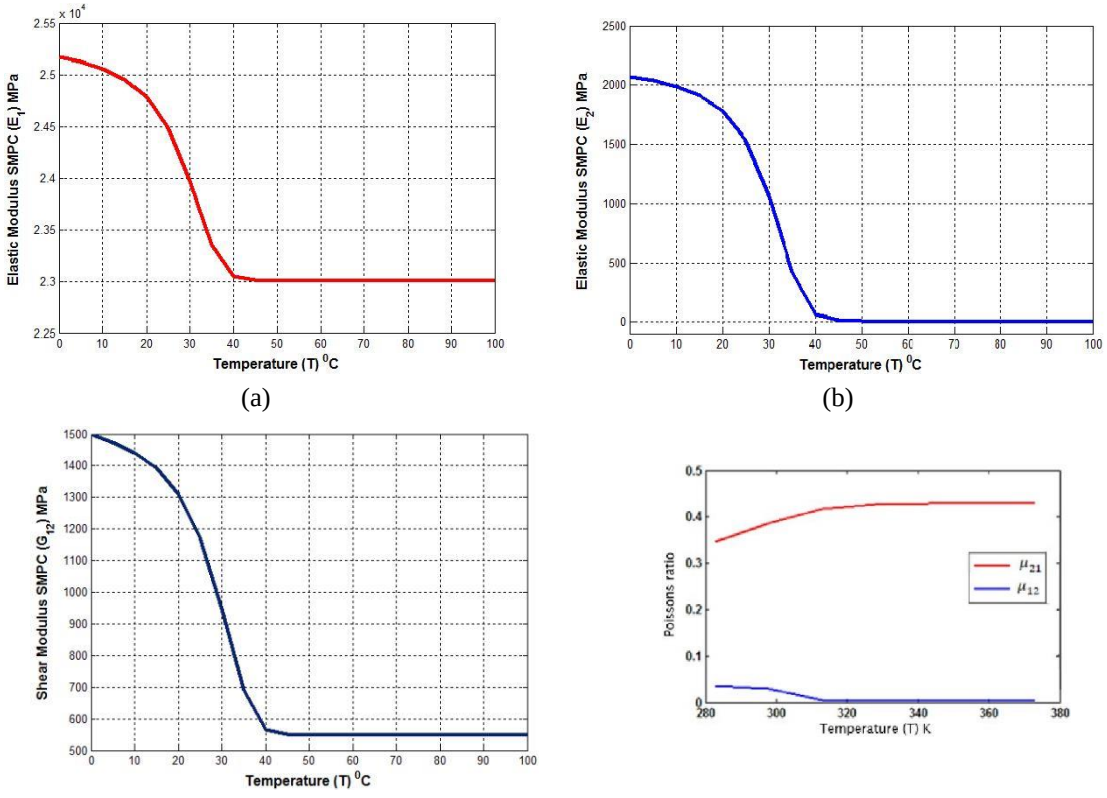

Fig. 2 Influence of variation of temperature on modulus: (a) longitudinal; (b) transverse; (c) shear modulus; and (d) Poissons ratio of SMPC

Table 2 Material properties of reinforcement (Shen *et al.* 2006)

Parameters	E_{f1}	E_{f2}	G_{f12}	μ_f	C
Values	2.3×10^5 MPa	8.2×10^{M}MPa	2.73×10^{M}MPa	0.25	0.2

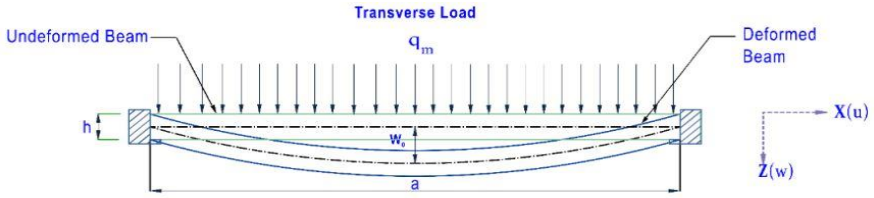

Fig. 3 Bending of 1D-beam SMPC Beam under Transverse Load with uniform temperature

2.3 Geometry configuration of SMPC Beam

An elastic SMPC beam with SMP as a matrix and carbon as reinforcement has been considered for the analysis to estimate the deflection of the 1D beam. The length of the beam is assumed to be *'a'* with thickness *'h'* as shown in Fig. 3 The deformation of a beam under the transverse load undergoes a deflection by Transverse Central Deflection (TCD) -W_0. In the present arrangement indicated in Fig. 3, a uniformly distributed transverse load (UDL) has been applied on the beam with clamped boundary condition. The carbon fiber reinforcement in the SMP matrix has been reinforced with consideration of uniform distribution along the matrix. The bonding between the fiber and matrix is assumed to be ideally perfect with no micro-buckling of fiber or delamination.

2.4 Displacement field model

Components of the model are evaluated for an arbitrary SMPC 1-D beam with modified displacement field components in 'x' and 'z' coordinates through the beam based on HSDT using C^0 continuity. This process has been adopted in Eq. (15), which eases the problems related to computations. (Reddy 2014)

$$\bar{u}(x,z) = \boldsymbol{u} + f_1(z)\Psi_x + f_2(z)\emptyset_x;\ \bar{w}(x,z) = \boldsymbol{w} \tag{15}$$

where $\boldsymbol{u}$, $\boldsymbol{w}$, and $\emptyset = \partial w/\partial x$ are displacement along mid-plane axis, displacement along transverse direction, rotation of normal to the mid-plane along 'y'- axis and slope along 'x'- axis, respectively. The parameter $f_1(z)$ and $f_2(z)$ are evaluated with Eq. (16).

$$f_1(z) = C_1 z - C_2 z^3,\ \ f_2(z) = -C_2 Z^3,\ \ \text{with}\ \ C_1 = 1,\ \ C_2 = \frac{4}{3}h^2 \tag{16}$$

Iso-parametric FEA has been adopted in an appropriate C^0 continuity to apply this theory with four degrees of freedom (DOFs) at individual node. This approach has been adopted in the formulation to reduce the cumbersome computations without affecting accuracy of the solution.

Displacement vector for the modified C^0 continuous model can be expressed as

$$\{\boldsymbol{q}\} = [\boldsymbol{u}\ \ \boldsymbol{w}\ \ \emptyset_{\boldsymbol{x}}\ \Psi_x]^T \tag{17}$$

2.5 Strain displacement relation

Total strain vector consists of linear strain (in terms of mid plane deformation, rotation of normal and higher order terms), non-linear strain (Von-Karman type) associated with the displacement for fiber reinforced polymer composites can be expressed as

$$\{\bar{\boldsymbol{\varepsilon}}\} = \{\bar{\boldsymbol{\varepsilon}}^{\boldsymbol{L}}\} + \{\bar{\boldsymbol{\varepsilon}}^{\boldsymbol{NL}}\} \tag{18}$$

where, $\{\bar{\boldsymbol{\varepsilon}}^{\boldsymbol{L}}\}$, $\{\bar{\boldsymbol{\varepsilon}}^{\boldsymbol{NL}}\}$ are linear strain and non-linear strain vectors, respectively. From Eq. (18), the linear strain tensor using HSDT can be written as

$$\bar{\boldsymbol{\varepsilon}}^{\boldsymbol{L}} = [B]\{\boldsymbol{q}\} \tag{19}$$

where [B] and $\{\boldsymbol{q}\}$ are the geometrical matrix and displacement field vector, respectively. Non-linear strain vector $\{\bar{\boldsymbol{\varepsilon}}^{\boldsymbol{NL}}\}$ can be written as

$$\bar{\boldsymbol{\varepsilon}}^{\boldsymbol{NL}} = \frac{1}{2}[A_{nl}]\{\emptyset_{\boldsymbol{nl}}\} \quad \text{where} \quad [A_{nl}] = \frac{1}{2}\left[\frac{\partial w}{\partial x}\right]^{T} \quad \text{and} \quad \{\emptyset_{\boldsymbol{nl}}\} = \left\{\frac{\partial w}{\partial x}\right\} \tag{20}$$

2.6 Stress-strain relation

The relation between stress $\{\bar{\boldsymbol{\sigma}}\}$ and strain for the plane-stress case using thermo-elastic constitutive model can be expressed as (Shegokar and Lal 2013)

$$\{\overline{\boldsymbol{\sigma}}\} = [Q]\{\bar{\boldsymbol{\varepsilon}}\} \tag{21}$$

$$\begin{Bmatrix}\overline{\boldsymbol{\sigma}_{\boldsymbol{x}}}\\ \bar{\boldsymbol{\tau}}_{\boldsymbol{xz}}\end{Bmatrix} = \begin{bmatrix}\overline{Q_{11}} & 0\\ 0 & \overline{Q_{55}}\end{bmatrix}\left\{\{\bar{\boldsymbol{\varepsilon}}^{\boldsymbol{L}}\} + \{\bar{\boldsymbol{\varepsilon}}^{\boldsymbol{NL}}\} - \{\bar{\boldsymbol{\varepsilon}}^{\boldsymbol{T}}\}\right\} \tag{22}$$

Where

$$\begin{aligned}\overline{Q_{11}} &= Q_{11}\sin^4\theta_k + 2(Q_{12}+2Q_{66})\cos^2\theta_k\cos^2\theta_k \text{ and } \overline{Q_{55}}\\ &= Q_{55}\cos^2\theta_k + Q_{44}\sin^2\theta_k\end{aligned} \tag{23a}$$

with

$$\begin{aligned}&Q_{11} = \frac{E_{C1}}{1-\mu_{12}\mu_{21}};\quad Q_{22} = \frac{E_{C12}}{1-\mu_{12}\mu_{21}};\quad Q_{12} = \frac{\mu_{C12}E_{C2}}{1-\mu_{12}\mu_{21}};\quad \mu_{21} = \frac{\mu_{C12}E_{C2}}{E_1};\\ &Q_{55} = G_{C12}; \qquad \text{and} \qquad Q_{44} = G_{C13}\end{aligned} \tag{23b}$$

Here θ_k is represented as fiber orientation. E_{C1} and E_{C2} are longitudinal, transverse respectively; G_{C12}, G_{C13} and G_{C23} are shear modulus; and μ_{C12} and μ_{C21} are Poisson's ratios.

2.7 Strain energy of SMPC beam

$$\Pi_{\boldsymbol{1}} = \boldsymbol{U_L} + \boldsymbol{U_{NL}} \tag{24}$$

Linear stain energy ($\boldsymbol{U_L}$) of the fiber reinforced polymer composite beam is written as

$$\boldsymbol{U_L} = \iint \frac{1}{2}\{\bar{\boldsymbol{\varepsilon}}^{\boldsymbol{L}}\}^T[Q]\{\bar{\boldsymbol{\varepsilon}}^{\boldsymbol{L}}\}\,dA = \iint \frac{1}{2}\{\bar{\boldsymbol{\varepsilon}}^{\boldsymbol{L}}\}^T[D]\{\bar{\boldsymbol{\varepsilon}}^{\boldsymbol{L}}\}\,dA \tag{25}$$

where [D] and $\{\bar{\boldsymbol{\varepsilon}}^{\boldsymbol{L}}\}$ are elastic stiffness matrix and linear strain vector, respectively.

Non-linear strain energy ($\boldsymbol{U_{NL}}$) of the fiber reinforced polymer composite beam can be represented as

$$\boldsymbol{U_{NL}} = \iint \frac{1}{2}\{\bar{\boldsymbol{\varepsilon}}^{\boldsymbol{L}}\}^T[D_1]\{\bar{\boldsymbol{\varepsilon}}^{\boldsymbol{NL}}\} + \frac{1}{2}\{\bar{\boldsymbol{\varepsilon}}^{\boldsymbol{NL}}\}^T[D_2]\{\bar{\boldsymbol{\varepsilon}}^{\boldsymbol{L}}\} + \frac{1}{2}\{\bar{\boldsymbol{\varepsilon}}^{\boldsymbol{NL}}\}^T[D_3]\{\bar{\boldsymbol{\varepsilon}}^{\boldsymbol{NL}}\}dA \tag{26}$$

where [D_1], [D_2] and [D_3] are elastic stiffness matrices of fiber reinforced polymer composite beam.

2.8 Work done due to external applied loading

Work done due to application of externally applied UDL can be stated as

$$\Pi_{\mathbf{3}} = \boldsymbol{W_q} = \iint \boldsymbol{q_m}\,(x,z)w\,dA \tag{27}$$

where, $q_m(x,z)$ is intensity of the applied uniformly distributed load.

2.9 Strain energy of the beam element

In the present work, a C^0 1-D Hermitian beam element with four degrees of freedom per node is employed (Shegokar and Lal 2013). Rewritten as this type of beam element geometry and the displacement vector.

$$\{\boldsymbol{q}\} = \sum_{i=1}^{NN} N_i\,\{\boldsymbol{q}\}_i\,; \qquad x = \sum_{i=1}^{NN} N_i\,x_i; \tag{28}$$

Where, N_i - interpolation function for ith node
$\{\boldsymbol{q}\}_i$ - vector of unknown displacements for ith node
NN - number of nodes per element
x_i - Cartesian coordinate

In order to calculate transverse displacement and slope, linear interpolation for axial displacement and rotation of normal and Hermite cubic interpolation functions are considered. Using FEM Eq. (28), Eq. (24) can be expressed a

$$\Pi_{\mathbf{1}} = \sum_{e=1}^{NE} \Pi_a^{(e)} = \sum_{e=1}^{NE} \left(\boldsymbol{U}_L^{(e)} + \boldsymbol{U}_{NL}^{(e)}\right) \tag{29}$$

where, NE and (e) denote the number of elements and elemental, respectively.

Eq. (29) can be further evaluated as

$$\Pi_{\mathbf{1}} = \frac{1}{2}\sum_{e=1}^{NE}\left[\{\boldsymbol{q}\}^{T(e)}[K_l + K_{nl}]^e\{\boldsymbol{q}\}^{(e)}\right] = \{\boldsymbol{q}\}^T[K_l + K_{nl}]\{\boldsymbol{q}\} \tag{30}$$

Here

$$[K_{nl}] = \frac{1}{2}[K_{nl1}] + [K_{nl2}] + \frac{1}{2}[K_{nl3}]$$

where $[K_l]$ is global linear matrix, $[K_{nl1}]$, $[K_{nl2}]$ and $[K_{nl3}]$ are non-linear stiffness matrices and $\{q\}$ is global displacement vector.

2.10 Work done due to external transverse load

Using FEM, Eq. (27) can be modified as (Shegokar and Lal 2013)

$$\Pi_{\mathbf{3}} = \sum_{e=1}^{NE}\Pi_3^{(e)} = \sum_{e=1}^{NE}\{\boldsymbol{q}\}^{(e)T}\{\boldsymbol{q_m}\}^{(e)} = \boldsymbol{q_m}\left\{0 \quad \frac{l_e}{2} \quad \frac{{l_e}^2}{12} \quad 0 \quad 0 \quad \frac{l_e}{2} \quad -\frac{{l_e}^2}{12}\right\}^{T(e)} \tag{31}$$

where, l_e is length of the beam element.

2.11 Governing equation of bending

Governing equation of the non-linear static analysis can be derived using Variational principle, which is generalized form of principle of virtual displacement. For the bending analysis, the minimization of first variation of total potential energy **Π (Π₁-Π₃)** with respect to displacement vector is given by

$$\partial(\Pi_{\mathbf{1}} - \Pi_{\mathbf{3}}) = 0 \tag{32}$$

By substituting the Eq. (29), Eq. (30) and Eq. (31). Resultant equation is obtained as

$$[K]\{\boldsymbol{q}\} = \{\boldsymbol{F}\} \tag{33a}$$

$$[K] = [K_l + K_{nl}] \tag{33b}$$

Stiffness matrix [*K*] consists of linear and non-linear plate stiffness matrices. Parameters {**q**} and {$\boldsymbol{F}$} are transverse deflection and force vector respectively.

The solution of Eq. (33) can be estimated through standard solution process such as direct iterative, incremental and/or Newton-Raphson method, etc. However, Newton Raphson method is one of the most recognized and widely used solution procedure due to fast convergence at higher amplitude.

2.12 Solution approach: *Newton Raphson method*

The system of non-linear static Eq. (33), can be written as (Reddy 2014)

$$[K(\{\boldsymbol{q}\})]\{\boldsymbol{q}\} = \{\boldsymbol{F}\} \tag{34}$$

where $[K(\{\boldsymbol{q}\})]$ is global non-linear stiffness matrix, which is function of unknown global nodal displacement vector $\{\boldsymbol{q}\}$ and global force vector $\{\boldsymbol{F}\}$. The procedure followed in this solution is stated as:

(1) Non-linear matrix is assumed to be zero and evaluate the nodal displacement by considering linear stiffness matrix.
(2) Nodal force vector is normalized.
(3) Force vector is amplified by C times in the condition of specified maximum force at the center of plate, so that resultant $\{\boldsymbol{F}\}$ will have force (C) at the maximum nodal force.
(4) Non-linear stiffness matrix is obtained for scaled up normalized force. Problem may again be treated as static equation with new modified stiffness matrix.
(5) Steps 2 to 4 are iterated by substituting $\{\boldsymbol{q}\}$ linear to non-linear $\{\boldsymbol{q_{nl}}\}$ in steps (1) and (2), to obtain converged displacement with prescribed accuracy of 10^{-3}.
(6) Iterate steps 1 to 5 for various values of C.

3. Results and discussion

User-defined program has been developed in MATLAB based on formulation discussed in section 2 to estimate TCD of shape memory polymer composites. SMPC under study is assumed to be a 1-D beam under the influence of uniformly distributed transverse load in static condition with consideration of uniform temperature across each element in SMPC beam. Temperature of beam is varied over a wide range that includes glass transition region of SMPC so that the deflection phenomenon with respect to uniform variation of temperature can be understood. TCD is calculated based on numerical analysis for numerous geometric parameters for instance different boundary conditions, aspect ratio of beam and number of laminas; and material parameters like volume fraction of carbon fiber, laminate stacking sequence with fiber orientation of SMPC for temperatures before and after T_g.

The comparison of linear and non-linear bending analysis clears the way to adopt non-linear approach so that the estimation of beam deflection under transverse load is improved. This paper considers Clamped beam at both edges (C-C), beam clamped at one edge and simply supported at another edge (C-S), cantilever beam – beam clamped at one edge and free at another (C-F), beam hinged at both edges (H-H) and beam hinged at one end and free at another (H-F) as boundary conditions. This provides a better understanding of temperature effect on beam under above mentioned boundary conditions. The evaluation of flexural analysis results transverse central deflection of SMPC beam also denoted by W_0, indicating the deflection at the midpoint of the beam under bending. σ_{xx} and σ_{xz} are longitudinal and shear stresses respectively, applied while uniformly distributed transverse loading of beam.

Elastic modulus of SMP has been presented in Fig. 1 for the range of temperature from 273 K to 373 K. T_g of SMP has been investigated to be 305 K with Poisson's ratio from 0.35 to 0.499 (Gu *et al*. 2019). Data required for modelling of composites are referred from the previous works by Gu *et al*. (2019) and Shen *et al*. (2006). Micro-mechanical modeling of developed composites is based on theory of volume averaging (Shen *et al*. 2006). Elaborate numerical solution for non-linear flexural deformation is presented for SMPC under the influence of uniformly distributed static load and dynamic temperature condition. Effective properties of SMP, carbon fiber and SMPC has been discussed in detail in previous section. Material properties varies drastically due

to dynamic property of glass transition region. Prior to the glass transition region, SMPC act as an elastic material with longitudinal modulus of 2.5 GPa whereas after the region it again act as elastic with modulus of 2.3 MPa, as shown in Fig. 2(a). Reduction of 8.62% has been noticed in the longitudinal modulus of SMPC in the glass transition region. Similarly, approximate decrement of 92.44% and 63.46% has been observed in transverse and shear modulus of SMPC respectively as described in Figs. 2(b) and (c). These properties indicates transition of deformation that can be estimated in the deflection under the influence of bending for dynamic temperature conditions.

3.1 Convergence study

Convergence study has been done to select the minimum number of elements (neL) to calculate the results without diluting the solutions. Two convergence analysis are performed, firstly convergence of non-linear TCD with respect to temperature at static load and another for TCD at discrete temperature for numerous number of elements. SMPC with 4 layers of symmetric - [0°/90°/90°/0°] arrangement and aspect ratio of 50 under the effect of uniformly distributed transverse load, has been considered in this study. Fig. 4 indicates variation of TCD for dynamic temperature condition from 273 K to 373 K with static load. It can be observed that as number of elements increase, solution also raises with gradual convergence as number elements reach 24.

In the second case, FEA has been performed to calculate non-linear TCD subjected to transverse load for constant temperature condition. Again, it can be inferred that, as neL increases,

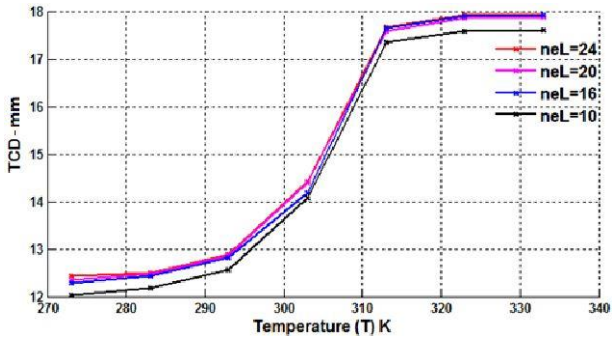

Fig. 4 Convergence of SMPC subjected to variable temperature and static load

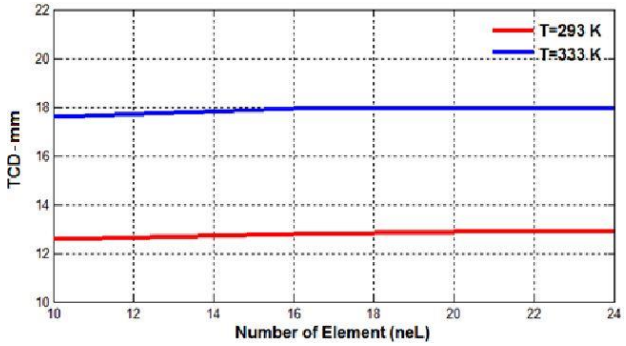

Fig. 5 Convergence of SMPC subjected to static load at constant temperature

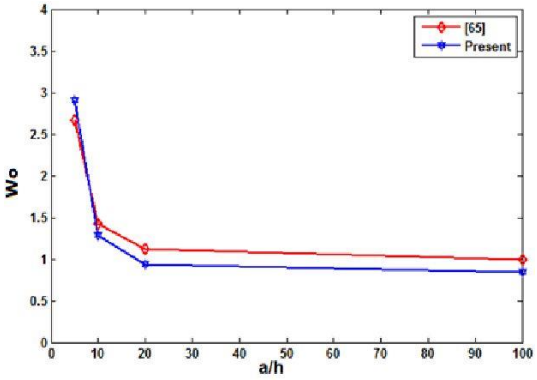

Fig. 6 Variation in non-dimensional TCD (w_o) with aspect ratio

magnitude of solution also increases, before it converges at 24 number of elements. Fig. 5 shows the study for two temperatures: 293 K and 333 K, which have similar convergence. Both the convergence tests have the similar results, indicating that the number of elements selected for FEM should be 24.

3.2 Validation study

Fig. 6 shows the accuracy and compatibility of the present analytical model with HSDT by validating it with work by Zia and Khan (2018) which presented its result with exponential shear deformation beam theory (ESDBT) and Timoshenko beam theory (TBT) at constant temperature. Fig. 6 indicate the nature of change for non-dimensional transverse central deflection (w_o) variation in laminated composite beam with the variation of beam aspect ratio (a/h), evaluated from Eq. (35). For validation purpose set of material properties selected are E_1 = 181 GPa, E_2 = 10.3 GPa, $G_{12} = G_{21}$ = 7.17 GPa, G_{23} = 2.87 GPa, $\nu_{12} = \nu_{13} = \nu_{12}$ = 0.25.

$$w_o = \frac{100wE_{c2}}{hr^4q_m} \tag{35}$$

here, r is aspect ratio (a/h) and w is TCD.

3.3 Parametric study

FEA performed on 1-D SMPC beam evaluates TCD under the influence of uniformly distributed transverse load for various parameters to highlight the effect of variations for various cases on beam, when subjected to variation of temperature across T_g. Parameters considered in present work include different boundary condition, geometric linearity and non-linearity, aspect ratio, ply orientation, and thickness. This is followed by the development of unit length deflection graph at different temperatures and volume fractions of reinforcement. Stress distribution diagram is also presented to understand the effect of applied transverse load at constant load.

3.3.1 Linear and non-linear study

Linear and non-linear study of 1-D four layered SMPC with [0°/90°/90°/0°] orientation,

subjected to UDL with both ends clamped is indicated in Fig. 7. Linear and non-linear TCD are evident in the cases of deflection which are indicated at two constant temperatures 283 K and 303 K. These two temperatures offer accuracy of analysis before and during the glass transition as described in Fig. 1. All the parametric study in this paper follows non-linearity (Von Karman) with SMPC having volume fraction of carbon fiber (V_f) as 10%, and beam aspect ratio as 50, apart from the one which performs parametric study of volume fraction of reinforcements.

3.3.2 Aspect ratio

Aspect ratio indicates the relation between length (a) and thickness (h) of the beam under study, considered to understand the effect of loading. Fig. 8 indicates the effect of variation for aspect ratio from 10 to 50 on TCD in the case of symmetric SMPC beam clamped at both ends subjected to dynamic temperature condition. Initially, when aspect ratio increases from 10 to 20, variation of deflection is limited which rise gradually as aspect ratio raises from 20 to 50. Each aspect ratio appropriately indicates the effect of temperature on the deflection, thus indicating that the selection of any aspect ratio would give satisfactory results. It has been observed that aspect ratio of 50 provides magnified and clear effect of glass transition region on deflection of SMPC beam. However, general observation again get verified over here that, deflection increases, as beam becomes thinner.

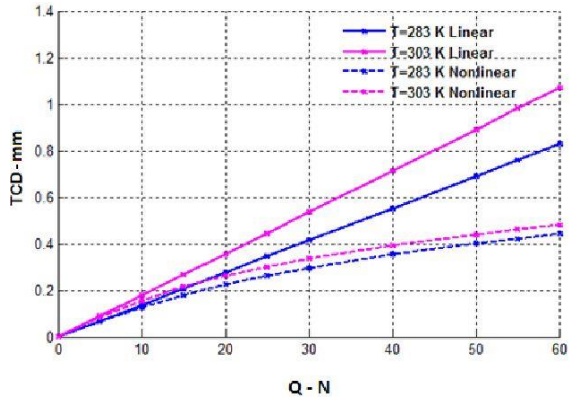

Fig. 7 Load-deflection variation in laminated composite beam for linear and nonlinear cases

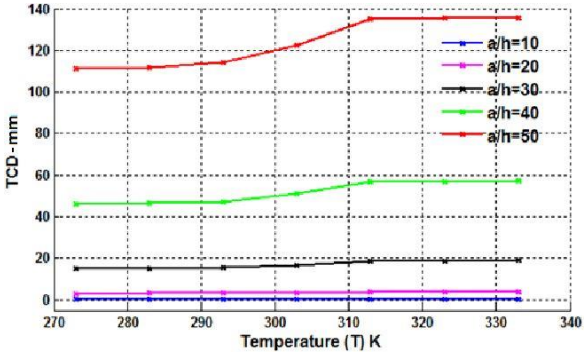

Fig. 8 Effect of variation of temperature and aspect ratio over TCD

3.3.3 Boundary Conditions (BCs)

SMPC beam with four layers has been considered to observe the effect of variation of temperature across T_g for different BCs. In this study, the beam has symmetric [0°/90°/90°/0°] orientation with aspect ratio of 50. Five distinct boundary conditions explained in this section, have been applied on the beam with UDL. Comparative results indicating the variation of temperature in each case is shown in Fig. 9. Initially below the initiation of glass transition region material behaves an elastic material, which is followed by the surge in the displacement due to the transition from elastic behavior to viscoelastic behavior in the ambience of temperature near to T_g. When the temperature crosses the glass transition region, material properties stabilize, highlighted in the constant displacement region. TCD is maximum for H-F boundary condition due to lesser constraint among all the considered BC, similarly, it is minimum for C-C because of more constraints.

3.3.4 Laminate stacking sequence with fiber orientation

Fiber orientation has quite significant effect on the material properties of composites. Table 3 indicates description of the schemes considered for the four layered SMPC subjected to uniformly distributed transverse load clamped at both ends. Fig. 10 indicates the effects of different stacking orientation on TCD. The deflections along the range of temperature are maximum in the anti-symmetric orientation of fiber laminates, whereas it is minimum for unidirectional laminates, which also correlates with the conventional laminate theory (Lal and Markad 2018). Eventually, effect of T_g is clearly demonstrated in all the orientations of stacking in terms of TCD for SMPC beam.

3.3.5 Number of layers

Effect of number of layers is studied with the consideration of constant beam aspect ratio of 30 with both edges clamped. Number of layers are varied from one to four in the cross-ply manner. Four cases of layup arrangements are [0°], [0°/90°], [0°/90°/0°] and [90°/0°/0°/90°]. In case of

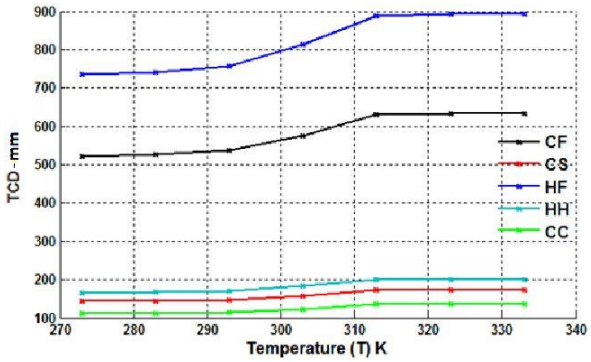

Fig. 9 SMPC subjected to variable temperature under different boundary conditions

Table 3 Types of laminate stacking

Symmetric	Anti-symmetric	Cross-ply	Angle-ply	Uni-directional
[0°/90°/90°/0°]	[45°/60°/-60°/-45°]	[0°/90°/0°/90°]	[45°/60°/90°/30°]	[0°/0°/0°/0°]

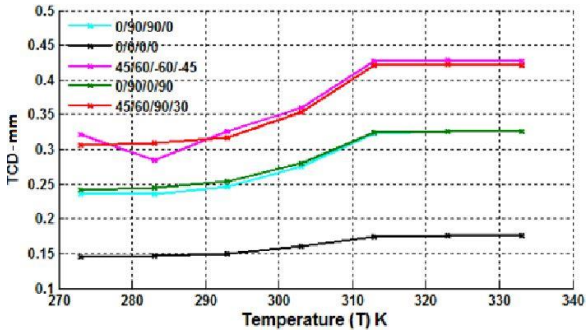

Fig. 10 SMPC subjected to variable temperature for various laminate stacking orientations

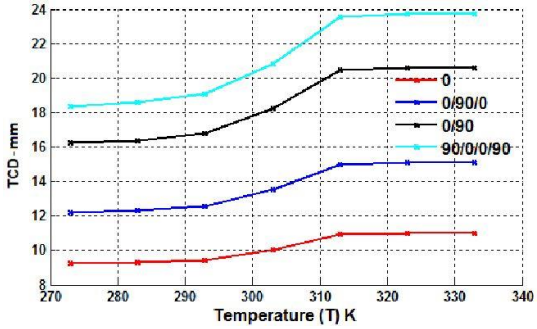

Fig. 11 Effect of number of layers on SMPC subjected to variable temperature

single layer SMPC, circular cross-section of carbon fiber is assumed to be equal to thickness of beam. Similarly, for the multiple layers, the summation of diameter for a corresponding number of layers is considered approximately equal to thickness of laminate. TCD is maximum for four layered SMPC [90°/0°/0°/90°] and minimum for one layered SMPC [0°], as demonstrated in Fig. 11. These results are in coherence with the one in Fig. 10, as single layered SMPC [0°] behave as unidirectional composite and four layered SMPC [90°/0°/0°/90°] behave as a symmetric one.

3.3.6 Deflection along length of beam

Deflection along unit length of a beam indicates the displacement of symmetric SMPC beam with [90°/0°/0°/90°] orientation at each element. Figs. 12 and 13 indicates relation between non-linear deflection (W_o) with respect to unit length for two parameters with the beam clamped at both ends. Flexural deformation of SMPC beam is maximum at midpoint of the unit length. Influence of temperature on deflection is shown in Fig. 12 for different temperatures. Trajectories of deflection agrees with the reduction of modulus as the temperature increases (Indicated in Fig. 1). Increase of displacement is shown with respect to temperature from 273 to 333 K, which encompasses the whole range of glass transition from 295.2 K (beginning of transition) to 318 K (end of transition), as highlighted in Figs. 1 and 2(a), (b) and (c).

Similarly, effect of volume fraction variation of reinforcement is described in Fig. 13 at 303 K. Temperature 303 K is considered to understand the effect of variation of volume fraction in glass transition phase of SMPC. Volume fraction of carbon fiber in SMP matrix varies from 10% to

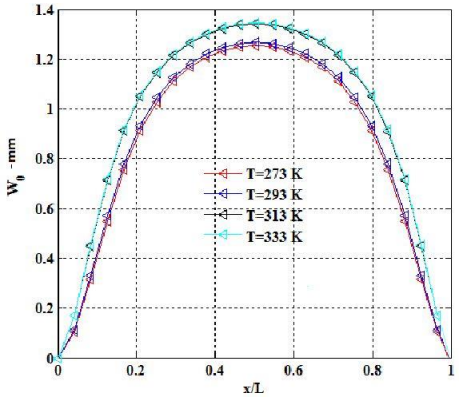

Fig. 12 Effect of variation in temperature on transverse deflection over unit length

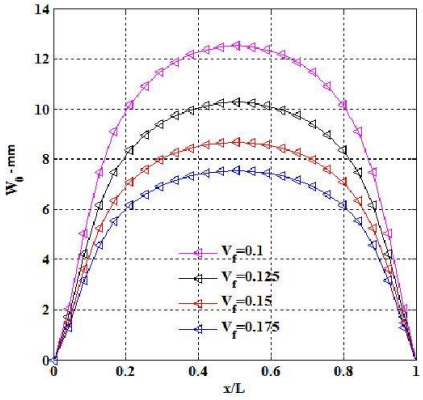

Fig. 13 Effect of variation in volume fraction of carbon fiber in SMPC

17.5%. Deflection of beam decreases with the rise of volume fraction due to increase of SMPC's stiffness. Hence, deflection of SMPC beam increases with increase of temperature, but if required it can be reduced with the increase of reinforcement in SMPC matrix. These combinations can offer wide range of deflection options as per the requirements that includes small (sensors) as well as large (deployable antennas) deformations shape recovery.

3.3.7 Stress distribution along thickness of SMPC

When SMPC beam is subjected to transverse load, beam displaces and it can be gauged with the help of Figs. 12 and 13. Stress distribution plot becomes essential to understand the effect of various stresses on the deflection of beam along thickness. Figs. 14(a)-(d) shows transverse displacement, longitudinal and shear stresses with respect to thickness of SMPC in transverse and longitudinal directions using FEM. SMPC of [0°/90°/0°/90°] orientation has been subjected to uniformly distributed transverse load at 303 K to highlight stress distribution in the vicinity of T_g. Longitudinal stress ($\boldsymbol{\sigma_{xx}}$) decreases linearly along the thickness SMPC and becomes zero at neutral axis, whereas shear stress ($\boldsymbol{\sigma_{xz}}$) have a parabolic stress distribution, indicating maximum stress at center and minimum at the edges. Thus, highlighting that transverse stress governs the bending phenomenon in the SMPC as longitudinal stress is linear in nature.

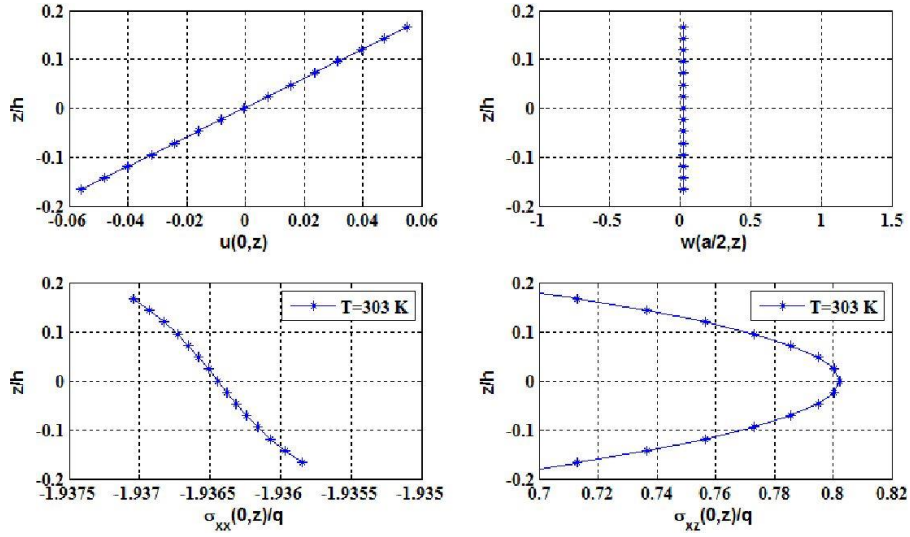

Fig. 14 Variation of (a) in plane displacement; (b) transverse displacement; (c) longitudinal stress; (d) shear stress along thickness of SMPC at 303 K

4. Conclusions

The present work deals with the non-linear flexural analysis of 1-D SMPC through a simplified C° continuity FEM based on HSDT. This work highlights the effect of glass transition temperature on the displacement of beam subjected to uniformly distributed transverse loading. Numerous parameters are varied to observe their effect on transverse central deflection for instance boundary conditions, volume fraction of reinforcements, aspect ratios, sequence of laminate stacking with fiber orientation and number layers for dynamic temperature conditions from 273 K to 373 K. Apart from this, deflection along unit length and stresses through thickness of SMPC beam have also been incorporated. Following conclusions have been inferred from the results of these parametric study considering dynamic temperature condition.

- Longitudinal, transverse and shear modulus of SMPC follows the behavior similar to SMP over a wide range of temperature, thereby demonstrating effect of glass transition region on SMPC.
- Due to decrement of modulus, corresponding variation of TCD is observed with respect to dynamic temperature condition for all the boundary conditions, aspect ratio, number of layers and orientation of laminate. These trajectories trail the similar pattern of constant deflection before the transition, followed with a surge in deflection during glass transition region and constant deflection after the transition region of SMPC. Thus, indicating that the approximate glass transition region of SMPC can be estimated, if it is under the influence of constant static load and dynamic temperature condition.
- TCD in the case of both clamped edges is minimum, whereas it is maximum for the beam hinged at one edge and free at another among all the BCs considered in the present work.
- Variation of aspect ratio is directly proportional to TCD in the glass transition region for aspect ratio from 10-50.
- Deflection is minimum for unidirectional orientation of laminate while it is maximum for

anti-symmetric laminates and if the number of layers is increased in cross-ply arrangement for constant aspect ratio of beam, then deflection increases with increase in number of layers.

Static temperature analysis has also been performed to plot deflection curve for unit length of beam under clamped boundary condition in order to highlight two conditions. First condition compares the deflection curve for variation of temperature from 273 K to 333 K, which reveals that as temperature increase across glass transition region, bending curve raises with maximum deflection at the center of unit length beam. This occurs due to the corresponding decrease in modulus of SMPC across glass transition region. Second condition compares the result for variation of volume fraction of reinforcement at constant temperature of 303 K. This indicates that if volume fraction increases in SMPC, then deflection reduces due to increase of stiffness in composites. Results are also presented to describe nature of stresses across thickness of SMPC at constant temperature, which signifies that deflection during the bending is regulated by transverse stress and the nature of shear stress distribution is parabolic in nature.

Thus, the present work explains the effect of T_g on flexural deflection of SMPC beam subjected to uniformly distributed load with the help of mentioned parametric studies. These results can facilitate in the further understanding of SMPC structures under large strain (deployable antennas), that can be helpful in its design and optimization using FEM.

References

Baghani, M., Naghdabadi, R., Arghavani, J. and Sohrabpour, S. (2012), "A constitutive model for shape memory polymers with application to torsion of prismatic bars", *J. Intel. Mater. Syst. Struct.*, **23**(2), 107-116. https://doi.org/10.1177/1045389X11431745

Baghani, M., Mohammadi, H. and Naghdabadi, R. (2014), "An analytical solution for shape-memory-polymer Euler–Bernoulli beams under bending", *Int. J. Mech. Sci.*, **84**, 84-90. https://doi.org/10.1016/j.ijmecsci.2014.04.009

Buehler, W.J., Gilfrich, J.V. and Wiley, R.C. (1963), "Effect of low-temperature phase changes on the mechanical properties of alloys near composition TiNi", *J. Appl. Phys.*, **34**(5), 1475-1477. https://doi.org/10.1063/1.1729603

Campbell, D., Mallick, K. and Lake, M. (2004), "A Study of the Compession Mechanics of Soft-Resin Composites", *Proceedings of the 45th AIAA/ASME/ASCE/AHS/ASC Structures, Structural Dynamics & Materials Conference*, CA, USA, April.

Cho, J.W., Kim, J.W., Jung, Y.C. and Goo, N.S. (2005), "Electroactive shape-memory polyurethane composites incorporating carbon nanotubes", *Macromol. Rapid Commun.*, **26**(5), 412-416. https://doi.org/10.1002/marc.200400492

Feldkamp, D.M. and Rousseau, I.A. (2010), "Effect of the Deformation Temperature on the Shape-Memory Behavior of Epoxy Networks", *Macromol. Mater. Eng.*, **295**(8), 726-734. https://doi.org/10.1002/mame.201000035

Gao, J., Chen, W., Yu, B., Fan, P., Zhao, B., Hu, J., Zhang, D., Fang, G. and Peng, F. (2019), "Effect of temperature on the mechanical behaviours of a single-ply weave-reinforced shape memory polymer composite", *Compos. Part B: Eng.*, **159**, 336-345. https://doi.org/10.1016/j.compositesb.2018.09.029

Ghosh, P. and Srinivasa, A. (2011), "Modeling and parameter optimization of the shape memory polymer response", *Mech. Mater.*

Ghosh, P., Reddy, J.N. and Srinivasa, A.R. (2013), "Development and implementation of a beam theory model for shape memory polymers", *Int. J. Solids Struct.*, **50**(3-4), 595-608. https://doi.org/10.1016/j.ijsolstr.2012.10.024

Gu, J., Leng, J. and Sun, H. (2017), "A constitutive model for amorphous shape memory polymers based on thermodynamics with internal state variables", *Mech. Mater.*, **111**, 1-14.

https://doi.org/10.1016/j.mechmat.2017.04.008
Gu, J., Xie, Z., Wang, S., Sun, H. and Zhang, X. (2018), "Thermo-mechanical modeling of woven fabric reinforced shape memory polymer composites", *Mech. Adv. Mater. Struct.*, **26**(12), 1042-1052. https://doi.org/10.1080/15376494.2018.1430266
Gu, J., Leng, J., Sun, H., Zeng, H. and Cai, Z. (2019), "Thermomechanical constitutive modeling of fiber reinforced shape memory polymer composites based on thermodynamics with internal state variables", *Mech. Mater.*, **130**, 9-19. https://doi.org/10.1016/j.mechmat.2019.01.004
Guo, J., Wang, Z., Tong, L. and Liang, W. (2016), "Effects of short carbon fibres and nanoparticles on mechanical, thermal and shape memory properties of SMP hybrid nanocomposites", *Compos. Part B: Eng.*, **90**, 152-159. https://doi.org/10.1016/j.compositesb.2015.12.010
Han, X.J., Dong, Z.Q., Fan, M.M., Liu, Y., Li, J.H., Wang, Y.F., Yuan, Q.J., Li, B.J. and Zhang, S. (2012), "pH-induced shape-memory polymers", *Macromol. Rapid Commun.*, **33**(12), 1055-1060. https://doi.org/10.1002/marc.201200153
Hassanzadeh-Aghdam, M.K., Ansari, R. and Mahmoodi, M.J. (2019), "Thermo-mechanical properties of shape memory polymer nanocomposites reinforced by carbon nanotubes", *Mech. Mater.*, **129**, 80-98. https://doi.org/10.1016/j.mechmat.2018.11.009
He, Y., Li, Y., Liu, Z. and Liew, K.M. (2017), "Buckling analysis and buckling control of thin films on shape memory polymer substrate", *Eur. J. Mech.-A/Solids*, **66**, 356-369. https://doi.org/10.1016/j.euromechsol.2017.08.006
Heuwers, B., Quitmann, D., Hoeher, R., Reinders, F.M., Tiemeyer, S., Sternemann, C., Tolan, M., Katzenberg, F. and Tiller, J.C. (2013), "Stress-Induced Stabilization of Crystals in Shape Memory Natural Rubber", *Macromol. Rapid Commun.*, **34**(2), 180-184. https://doi.org/10.1002/marc.201200594
Jani, J.M., Leary, M., Subic, A. and Gibson, M.A. (2014), "A review of shape memory alloy research, applications and opportunities", *Mater. Des.*, **56**, 1078-1113. https://doi.org/10.1016/j.matdes.2013.11.084
Kausar, A. (2016), "Nanodiamond tethered epoxy/polyurethane interpenetrating network nanocomposite: Physical properties and thermoresponsive shape-memory behavior", *Int. J. Polym. Anal. Characteriz.*, **21**(4), 348-358. https://doi.org/10.1080/1023666X.2016.1156911
Koerner, H., Strong, R.J., Smith, M.L., Wang, D.H., Tan, L.S., Lee, K.M., White, T.J. and Vaia, R.A. (2013), "Polymer design for high temperature shape memory: Low crosslink density polyimides", *Polym.*, **54**(1), 391-402. https://doi.org/10.1016/j.polymer.2012.11.007
Lal, A. and Markad, K. (2018), "Deflection and stress behaviour of multi-walled carbon nanotube reinforced laminated composite beams", *Comput. Concrete, Int. J.*, **22**(6), 501-514. https://doi.org/10.12989/cac.2018.22.6.501
Lal, A., Singh, B.N. and Kumar, R. (2007), "Natural frequency of laminated composite plate resting on an elastic foundation with uncertain system properties", *Struct. Eng. Mech., Int. J.*, **27**(2), 199-222. https://doi.org/10.12989/sem.2007.27.2.199
Lan, X., Liu, Y., Lv, H., Wang, X., Leng, J. and Du, S. (2009), "Fiber reinforced shape-memory polymer composite and its application in a deployable hinge", *Smart Mater. Struct.*, **18**(2), 024002. https://doi.org/10.1088/0964-1726/18/2/024002
Lan, X., Liu, L., Liu, Y., Leng, J. and Du, S. (2014), "Post microbuckling mechanics of fibre-reinforced shape-memory polymers undergoing flexure deformation", *Mech. Mater.*, **72**, 46-60. https://doi.org/10.1016/j.mechmat.2013.05.012
Lendlein, A., Jiang, H., Jünger, O. and Langer, R. (2005), "Light-induced shape-memory polymers", *Nature*, **434**(7035), 879-882. https://doi.org/10.1038/nature03496
Leng, J., Lan, X., Liu, Y. and Du, S. (2011), "Shape-memory polymers and their composites: stimulus methods and applications", *Progress Mater. Sci.*, **56**(7), 1077-1135. https://doi.org/10.1016/j.pmatsci.2011.03.001
Li, F., Liu, L., Lan, X., Zhou, X., Bian, W., Liu, Y. and Leng, J. (2016), "Preliminary design and analysis of a cubic deployable support structure based on shape memory polymer composite", *Int. J. Smart Nano Mater.*, **7**(2), 106-118. https://doi.org/10.1080/19475411.2016.1212948
Li, F., Scarpa, F., Lan, X., Liu, L., Liu, Y. and Leng, J. (2019), "Bending shape recovery of unidirectional

carbon fiber reinforced epoxy-based shape memory polymer composites", *Compos. Part A: Appl. Sci. Manuf.*, **116**, 169-179. https://doi.org/10.1016/j.compositesa.2018.10.037

Liu, Y., Gall, K., Dunn, M.L. and McCluskey, P. (2003), "Thermomechanical recovery couplings of shape memory polymers in flexure", *Smart Mater. Struct.*, **12**(6), 947. https://doi.org/10.1088/0964-1726/12/6/012

Liu, Y., Du, H., Liu, L. and Leng, J. (2014), "Shape memory polymers and their composites in aerospace applications: a review", *Smart Mater. Struct.*, **23**(2), 023001. https://doi.org/10.1088/0964-1726/23/2/023001

Lu, J., Arsalan, A., Dong, Y., Zhu, Y., Qian, C., Wang, R., Cuilan, C., Fu, Y., Ni, Q.Q. and Ali, K.N. (2017), "Shape memory effect and recovery stress property of carbon nanotube/waterborne epoxy nanocomposites investigated via TMA", *Polym. Test.*, **59**, 462-469. https://doi.org/10.1016/j.polymertesting.2017.03.001

Mahieux, C.A. and Reifsnider, K.L. (2001), "Property modeling across transition temperatures in polymers: a robust stiffness–temperature model", *Polymer*, **42**(7), 3281-3291. https://doi.org/10.1106/009524402022348

Mohr, R., Kratz, K., Weigel, T., Lucka-Gabor, M., Moneke, M. and Lendlein, A. (2006), "Initiation of shape-memory effect by inductive heating of magnetic nanoparticles in thermoplastic polymers", *Proceedings of the National Academy of Sciences*, **103**(10), 3540-3545.

Mu, T., Liu, L., Lan, X., Liu, Y. and Leng, J. (2018), "Shape memory polymers for composites", *Compos. Sci. Technol.*, **160**, 169-198. https://doi.org/10.1016/j.compscitech.2018.03.018

Nurly, H., Yan, Q., Song, B. and Shi, Y. (2019), "Effect of carbon nanotubes reinforcement on the polyvinyl alcohol–polyethylene glycol double-network hydrogel composites: A general approach to shape memory and printability", *Eur. Polym. J.*, **110**, 114-122. https://doi.org/10.1016/j.eurpolymj.2018.11.006

Oh, S.H., Kang, S.G. and Lee, J.H. (2006), "Degradation behavior of hydrophilized PLGA scaffolds prepared by melt-molding particulate-leaching method: comparison with control hydrophobic one", *J. Mater. Sci.: Mater. Med.*, **17**(2), 131-137. https://doi.org/10.1007/s10856-006-6816-2

Patel, K.K. and Purohit, R. (2019), "Improved shape memory and mechanical properties of microwave-induced thermoplastic polyurethane/Graphene nanoplatelets composites", *Sensors Actuat. A: Phys.*, **285**, 17-24. https://doi.org/10.1016/j.sna.2018.10.049

Pearce, G.M.K., Mukkavilli, A., Chowdhury, N.T., Lim, S.H., Prusty, B.G., Crosky, A. and Kelly, D.W. (2019), "Strain Invariant Failure Theory–Part 1: An extensible framework for predicting the mechanical performance of fibre reinforced polymer composites", *Compos. Struct.*, **209**, 1022-1034. https://doi.org/10.1016/j.compstruct.2018.03.084

Poilane, C., Delobelle, P., Lexcellent, C., Hayashi, S. and Tobushi, H. (2000), "Analysis of the mechanical behavior of shape memory polymer membranes by nanoindentation, bulging and point membrane deflection tests", *Thin Solid Films*, **379**(1-2), 156-165. https://doi.org/10.1016/S0040-6090(00)01401-2

Qi, H.J., Nguyen, T.D., Castro, F., Yakacki, C.M. and Shandas, R. (2008), "Finite deformation thermo-mechanical behavior of thermally induced shape memory polymers", *J. Mech. Phys. Solids*, **56**(5), 1730-1751. https://doi.org/10.1016/j.jmps.2007.12.002

Quade, D., Jana, S., Morscher, G., Kannan, M. and McCorkle, L. (2018), "The effects of fiber orientation and adhesives on tensile properties of carbon fiber reinforced polymer matrix composite with embedded nickel-titanium shape memory alloys", *Compos. Part A: Appl. Sci. Manuf.*, **114**, 269-277. https://doi.org/10.1016/j.compositesa.2018.08.019

Quitmann, D., Gushterov, N., Sadowski, G., Katzenberg, F. and Tiller, J.C. (2014), "Environmental memory of polymer networks under stress", *Adv. Mater.*, **26**(21), 3441-3444. https://doi.org/10.1002/adma.201305698

Reddy, J.N. (2014), *An Introduction to Nonlinear Finite Element Analysis: With Applications to Heat Transfer, Fluid Mechanics, and Solid Mechanics*, OUP, Oxford, UK.

Rodriguez, J.N., Yu, Y.J., Miller, M.W., Wilson, T.S., Hartman, J., Clubb, F.J., Gentry, B. and Maitland, D.J. (2012), "Opacification of shape memory polymer foam designed for treatment of intracranial aneurysms", *Annals Biomed. Eng.*, **40**(4), 883-897. https://doi.org/10.1007/s10439-011-0468-1

Shegokar, N.L. and Lal, A. (2013), "Stochastic nonlinear bending response of piezoelectric functionally graded beam subjected to thermoelectromechanical loadings with random material properties", *Compos. Struct.*, **100**, 17-33. https://doi.org/10.1142/S2047684117500208

Shen, G.L., Hu, G. and Liu, B. (2006), *Mechanics of Composite Materials*, Science and Technology, Beijing, China.

Shi, G., Lam, K.Y. and Tay, T.E. (1998), "On efficient finite element modeling of composite beams and plates using higher-order theories and an accurate composite beam element", *Compos. Struct.*, **41**(2), 159-165. https://doi.org/10.1016/j.ijsolstr.2007.11.005

Su, X. and Peng, X. (2018), "A 3D finite strain viscoelastic constitutive model for thermally induced shape memory polymers based on energy decomposition", *Int. J. Plastic.*, **110**, 166-182. https://doi.org/10.1016/j.ijplas.2018.07.002

Vernon, L.B. and Vernon, H.M. (1941), "Process of Manufacturing Articles of Thermoplastic Synthetic Resins", US Patent issued in March 1941.

Wang, Z.D. and Li, Z.F. (2011), "Theoretical analysis of the deformation of SMP sandwich beam in flexure", *Arch. Appl. Mech.*, **81**(11), 1667-1678. https://doi.org/10.1007/s00419-011-0510-7

Wang, Z., Li, Z., Xiong, Z. and Wang, L. (2010), "Theoretical studies on microbuckling mode of elastic memory composites", *Acta Mechanica Solida Sinica*, **23**(1), 20-28. https://doi.org/10.1016/S0894-9166(10)60003-1

Wang, E., Dong, Y., Islam, M.Z., Yu, L., Liu, F., Chen, S., Qi, X., Zhu, Y., Fu, Y., Xu, Z. and Hu, N. (2019a), "Effect of graphene oxide-carbon nanotube hybrid filler on the mechanical property and thermal response speed of shape memory epoxy composites", *Compos. Sci. Technol.*, **169**, 209-216. https://doi.org/10.1016/j.compscitech.2018.11.022

Wang, E., Wu, Y., Islam, M.Z., Dong, Y., Zhu, Y., Liu, F., Fu, Y., Xu, Z. and Hu, N. (2019b), "A novel reduced graphene oxide/epoxy sandwich structure composite film with thermo-, electro-and light-responsive shape memory effect", *Mater. Lett.*, **238**, 54-57. https://doi.org/10.1016/j.matlet.2018.11.138

Ware, T., Simon, D., Hearon, K., Liu, C., Shah, S., Reeder, J., Khodaparast, N., Kilgard, M.P., Maitland, D.J., Rennaker, R.L. and Voit, W.E. (2012), "Three-Dimensional Flexible Electronics Enabled by Shape Memory Polymer Substrates for Responsive Neural Interfaces", *Macromol. Mater. Eng.*, **297**(12), 1193-1202. https://doi.org/10.1002/mame.201200241

Westbrook, K.K., Kao, P.H., Castro, F., Ding, Y. and Qi, H.J. (2011), "A 3D finite deformation constitutive model for amorphous shape memory polymers: a multi-branch modeling approach for nonequilibrium relaxation processes", *Mech. Mater.*, **43**(12), 853-869. https://doi.org/10.1016/j.mechmat.2011.09.004

Xie, T. and Rousseau, I.A. (2009), "Facile tailoring of thermal transition temperatures of epoxy shape memory polymers", *Polymer*, **50**(8), 1852-1856. https://doi.org/10.1016/j.polymer.2009.02.035

Yang, D. (2000), "Shape memory alloy and smart hybrid composites—advanced materials for the 21st Century", *Mater. Des.*, **21**(6), 503-505. https://doi.org/10.1016/S0261-3069(00)00008-X

Zeng, H., Leng, J., Gu, J. and Sun, H. (2018), "A thermoviscoelastic model incorporated with uncoupled structural and stress relaxation mechanisms for amorphous shape memory polymers", *Mech. Mater.*, **124**, 18-25. https://doi.org/10.1016/j.mechmat.2018.05.010

Zhang, C.S. and Ni, Q.Q. (2007), "Bending behavior of shape memory polymer based laminates", *Compos. Struct.*, **78**(2), 153-161. https://doi.org/10.1016/j.compstruct.2005.08.029

Zhang, J., Dui, G. and Liang, X. (2018), "Revisiting the micro-buckling of carbon fibers in elastic memory composite plates under pure bending", *In. J. Mech. Sci.*, **136**, 339-348. https://doi.org/10.1016/j.ijmecsci.2017.12.018

Zhou, J., Li, H., Liu, W., Dugnani, R., Tian, R., Xue, W., Chen, Y., Guo, Y., Duan, H. and Liu, H. (2016), "A facile method to fabricate polyurethane based graphene foams/epoxy/carbon nanotubes composite for electro-active shape memory application", *Compos. Part A: Appl. Sci. Manuf.*, **91**, 292-300. https://doi.org/10.1016/j.compositesa.2016.10.021

Zia, Y.B. and Khan, A.A. (2018), "Comparison of various higher order shear deformation theories for static and modal analysis of composite beam", *Proceedings of IOP Conference Series: Materials Science and Engineering*, **377**, 012170. https://doi.org/10.1088/1757-899X/377/1/012170